Silver Nanowires as Surface Plasmon Resonators

Harald Ditlbacher,[1] Andreas Hohenau,[1] Dieter Wagner,[2] Uwe Kreibig,[2] Michael Rogers,[3] Ferdinand Hofer,[3] Franz R. Aussenegg,[1] and Joachim R. Krenn[1]

[1]*Institute of Physics, Karl-Franzens-University, 8010 Graz, Austria*
[2]*Physikalisches Institut I.A, RWTH, 52074 Aachen, Germany*
[3]*Austrian Centre for Electron Microscopy and Nanoanalysis, 8010 Graz, Austria*

(Received 6 September 2005; published 16 December 2005)

We report on chemically prepared silver nanowires (diameters around 100 nm) sustaining surface plasmon modes with wavelengths shortened to about half the value of the exciting light. As we find by scattered light spectroscopy and near-field optical microscopy, the nonradiating character of these modes together with minimized damping due to the well developed wire crystal structure gives rise to large values of surface plasmon propagation length and nanowire end face reflectivity of about 10 μm and 25%, respectively. We demonstrate that these properties allow us to apply the nanowires as efficient surface plasmon Fabry-Perot resonators.

DOI: 10.1103/PhysRevLett.95.257403 PACS numbers: 78.67.Lt, 73.20.Mf, 73.22.Lp, 78.66.−w

The integration of optics with nanotechnology is hindered by the lack of subwavelength photonic elements. Surface plasmons—coupled excitations of light and electrons at a metal surface—are a potential solution to this problem, as they allow the concentration of light to subwavelength volumes [1]. Recent advances in plasmonics have demonstrated surface plasmon waveguiding and optical addressing and, thus, the feasibility of integrated plasmon optics. Waveguiding in μm-wide metal thin films [2–4] and nanowires [5–9] and passive [10] and dynamic control [11] thereof has been shown. Here we report the experimental realization of Fabry-Perot–type plasmon resonators by chemically prepared silver wires with ~100 nm cross-section diameters and lengths up to about 20 μm. Our resonators rely on specific plasmon modes with wavelengths considerably shorter than the exciting light wavelength. These modes are not radiation damped and lead, thus, to unexpectedly large propagation lengths. Besides laying the foundation for wavelength selective devices, nanowire resonators might, therefore, enable improved spatial resolution in plasmon-based photonic circuitry.

Provided that the wire end faces reflect an incident surface plasmon, a nanowire can be turned into a surface plasmon resonator. Then resonator modes, i.e., standing surface plasmon waves along the nanowire axis, exist whenever an integer of half the surface plasmon wavelength equals the wire length. The maximum achievable resonator length is, however, limited by the metallic damping of the surface plasmon mode [12]. We investigate chemically prepared silver nanowires with a well defined crystal and surface structure, thereby minimizing surface plasmon damping due to scattering at roughness, domain boundaries, or defects. The nanowires are produced by a chemical reduction method of silver ions in an aqueous electrolyte solution. The fabrication process yields nanowires with cross-section diameters of 13–130 nm and lengths up to 70 μm [13]. High resolution transmission electron microscopy reveals the nanowires to consist of a lattice aligned bundle of five monocrystalline rods of a triangular cross section forming an almost regular pentagonal cross section [13]. Casting the purified electrolyte on a glass slide and letting it dry under ambient conditions yields well separated individual wires on the slide. One such wire is shown in Fig. 1.

Surface plasmon propagation along a nanowire can be straightforwardly demonstrated by local optical excitation [7]. We focus a laser beam under normal incidence with respect to the substrate plane with a microscope objective (60 ×, numerical aperture of 1.4) onto one end face (input end) of a 18.6 μm long nanowire with a diameter of 120 nm; see Fig. 2(a). The laser wavelength is 785 nm, and the polarization is oriented along the nanowire axis.

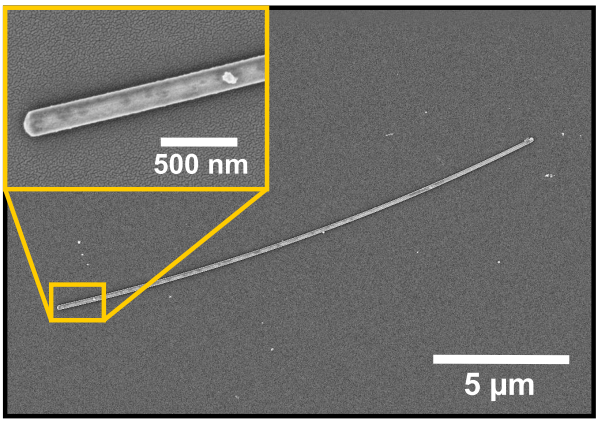

FIG. 1 (color online). Scanning electron micrographs of a 18.6 μm long silver nanowire. The wire diameter of 120 nm was independently determined by measuring the height of the nanowire by atomic force microscopy. In the image, the wire diameter is larger, as the sample was sputtered with 30 nm gold to provide electric conductivity for electron microscopy imaging.

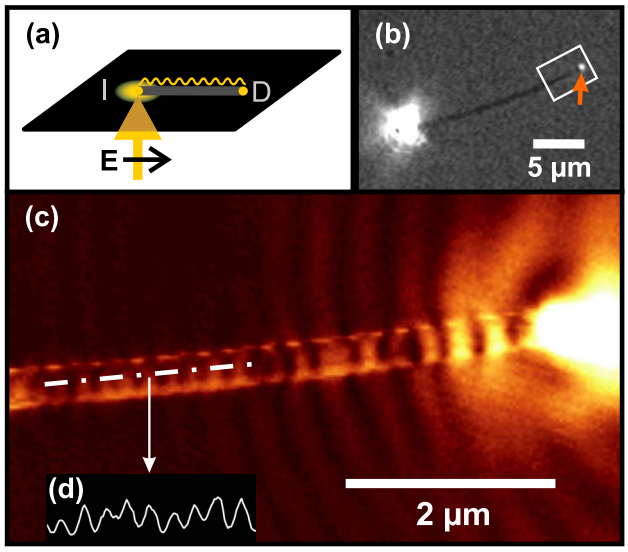

FIG. 2 (color online). Surface plasmon propagation along the 18.6 μm long silver nanowire in Fig. 1. (a) Sketch of optical excitation; I is input and D is distal end of the wire. (b) Microscopic image—the bright spot to the left is the focused exciting light. The arrow indicates light scattered from the distal wire end. (c) SNOM image—the image area corresponds to the white box in (b). (d) 2 μm long cross-cut along the chain dotted line in (c).

Part of the incident laser intensity is scattered into a surface plasmon mode, which propagates towards the distal end of the wire. There, part of the plasmon intensity is scattered to light, which can be detected with a conventional optical microscope, as shown in the image acquired with a charge-coupled-device (CCD) camera in Fig. 2(b). For light field polarization normal to the wire axis, the distal end remains dark.

Light emission from the nanowire in Fig. 2(b) is constricted to the distal end face due to the strongly bound character of the surface plasmon field, which couples to far field light only at wire discontinuities. Direct imaging of the surface plasmon field along the nanowire can, thus, be accomplished only by a near-field technique such as scanning near-field optical microscopy (SNOM) [14,15]. While maintaining the same excitation scheme as above, the optical image is now acquired by a sharp glass fiber tip raster scanned over the sample in a distance of a few nanometers. This distance is monitored by measuring the shear force between tip and sample [16] and maintained by a piezoelectric actuator. A SNOM image over the sample area defined by the box in Fig. 2(b) is shown in Fig. 2(c). The image reveals the modulation of the surface plasmon near field along the nanowire due to plasmon reflection at the distal wire end face. Similar patterns have been observed before on metal stripes with widths ranging from a few μm down to 200 nm [8–10]. In all these cases, surface plasmon wavelengths (2 times the observed modulation pitch) closely matching those expected for a flat extended surface were found. For the present case of a silver nanowire with a diameter of 120 nm, however, the surface plasmon wavelength is 414 nm, which is considerably shorter than the exciting light wavelength of 785 nm. The ratio of these two wavelengths shows that the surface plasmon mode cannot directly couple to far field light neither in air nor in the glass substrate (refractive index 1.5). This finding implies that plasmon propagation along the wire is not radiation damped.

For closer analysis, we turn to spectroscopy, analyzing light scattered from both nanowire end faces as a function of wavelength. Therefore, we replace the laser by a halogen lamp as a white light source and extend the CCD camera setup for acquiring optical spectra in combination with a monochromator. The scattered light is collected by a microscope objective (50 ×, numerical aperture of 0.85). For suppression of excitation light, we use a dark field technique, illuminating the sample under total internal reflection through a glass prism optically coupled to the substrate glass slide [Fig. 3(a)]. Since white light cannot be focused as tightly as a laser beam, we illuminate the nanowire uniformly (focus diameter 1 mm). For two reasons,

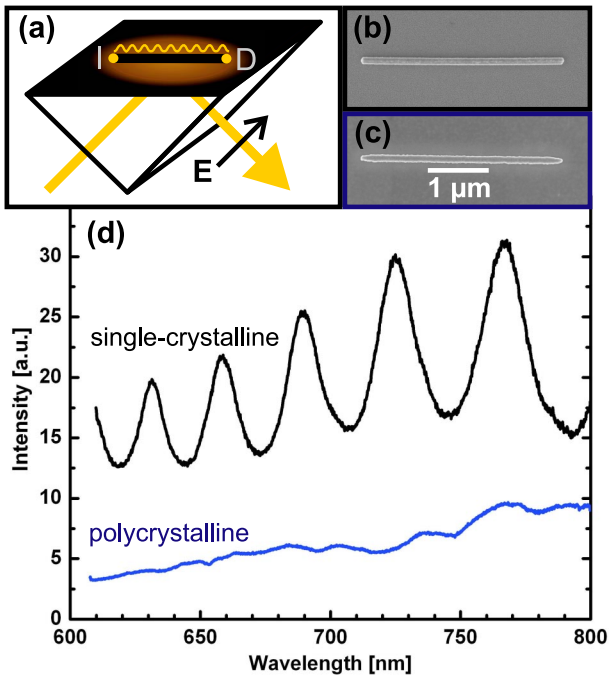

FIG. 3 (color online). Scattered light spectra of 3.3 μm long silver nanowires, diameter 90 nm. (a) Sketch of optical excitation. The exciting light propagation direction projected onto the substrate plane is parallel to the nanowire axis defining an input (I) and a distal end (D), and the polarization is fixed in the plane of incidence. (b),(c) Scanning electron micrographs of a chemically and an electron-beam lithographically fabricated silver nanowire, respectively. (d) Scattered light spectra from the distal nanowire end face of the chemically fabricated wire (single-crystalline, upper curve) and the lithographically fabricated wire (polycrystalline, lower curve).

the light field nevertheless couples to the surface plasmon mode (with a noteworthy efficiency) only at one end face of the wire. First, as mentioned above, the surface plasmon can be excited only at the end faces of the wire. Second, the exciting evanescent light field propagates along the substrate/air interface parallel to the wire axis [compare Fig. 3(a)], thereby defining an input and a distal end. We verified the latter point by focusing laser light selectively on either the input or the distal wire end. Indeed, a plasmon mode was observed only when exciting the input end.

The upper curve in Fig. 3(d) shows the spectrum taken from the distal end of a 3.3 μm long nanowire [diameter 90 nm, see Fig. 3(b)]. This and all spectra discussed in the following are corrected for background signals originating from scattering of the bare substrate. The scattered light intensity is modulated as a function of wavelength, with the distinct line shape of Fabry-Perot resonator modes [17]. This is indicative of multiple reflections of the surface plasmon wave and, thus, a plasmon propagation length considerably larger than the wire length. For comparison, we applied electron-beam lithography [18] to fabricate a nanowire geometrically corresponding to the wire in Fig. 3(b). This sample [Fig. 3(c)] is polycrystalline and shows some surface roughness. The corresponding scattered light spectrum [lower curve in Fig. 3(d)] displays no regular signal modulation. This underlines the importance of a highly ordered crystalline structure of the nanowire to achieve a large surface plasmon propagation length.

Scattered light spectra taken from both the input and distal ends of nanowires with lengths of 8.3 μm (diameter 75 nm) and 18.6 μm (diameter 120 nm) are shown in Figs. 4(a) and 4(b), respectively. The analysis of these spectra reveals the following aspects. First, with increasing wire length, the linewidth of the Fabry-Perot resonator modes increases. This is because the losses of the surface plasmon mode increase with the wire length. Second, signal minima from the input end correspond to maxima from the distal wire end and vice versa. This finding strongly corroborates the interpretation of optically excited nanowires as Fabry-Perot resonators. The scattered light intensities from the input and distal nanowire ends correspond to the transmission and reflection intensities of a resonator constituted by two mirrors facing each other. We note that this result confirms our former assumption that surface plasmons are not directly excited by the incident light at the distal wire end with a noteworthy efficiency. Third, the modulation depth of the spectra varies with both wavelength (reflecting the wavelength dependent dielectric function of silver) and nanowire length. The relative modulation depth $\Delta I/I_{\mathrm{min}}$ [see Fig. 4(b)] is given by the intensity related parameters propagation loss A and end face reflectivity R (Ref. [17]),

$$\frac{\Delta I}{I_{\mathrm{min}}} = \frac{4RA}{(1-RA)^2}. \qquad (1)$$

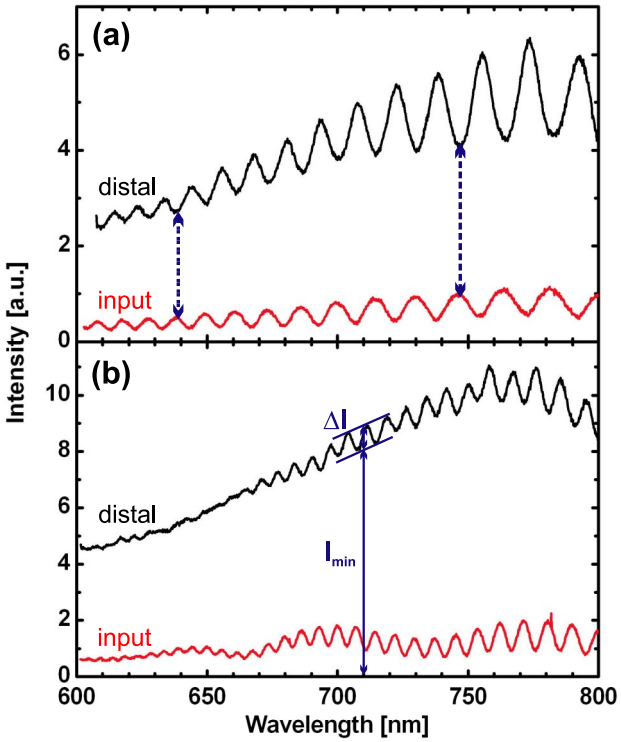

FIG. 4 (color online). Scattered light spectra of the nanowire distal and input end faces. (a) Spectra for a 8.3 μm long silver nanowire, diameter 75 nm. The vertical arrows highlight the spectral match between signal maxima and minima at the input and the distal end faces, respectively. (b) Spectra for a 18.6 μm long nanowire, diameter 120 nm. The arrows define ΔI and I_{min}.

As the propagation loss is defined as $A = e^{-L/l}$ (L is nanowire length, l is surface plasmon propagation length), the values for R and l can be deduced by analysis of the spectral data from nanowires of different lengths.

We extracted the relative modulation depth $\Delta I/I_{\mathrm{min}}$ around a light wavelength of 785 nm from the spectra of five nanowires with lengths ranging from 3.7 to 18.6 μm. The diameters of all these nanowires are within the range 110 ± 15 nm. Figure 5 shows the measured $\Delta I/I_{\mathrm{min}}$ values (squares) plotted against the length of the corresponding wire. The solid line is a fit of expression (1) to the data points, yielding values of $R = 0.25 \pm 0.01$ and $l = 10.1 \pm 0.4$ μm. We note that the uncertainty in the value of the propagation length (0.4 μm) does not include the uncertainty in the diameter of the wires. While the wire diameter is expected to affect the plasmon propagation length, we tried to minimize this effect by selecting nanowires with closely matching diameters.

The value for the propagation length of surface plasmons in chemically prepared silver nanowires is well above the propagation lengths on metal nanowires reported before [9]. This result can be assigned mainly to the well developed crystal and surface structure of our chemically fabricated samples. In addition, however, we deal with a plasmon mode that does not lose energy via radiation

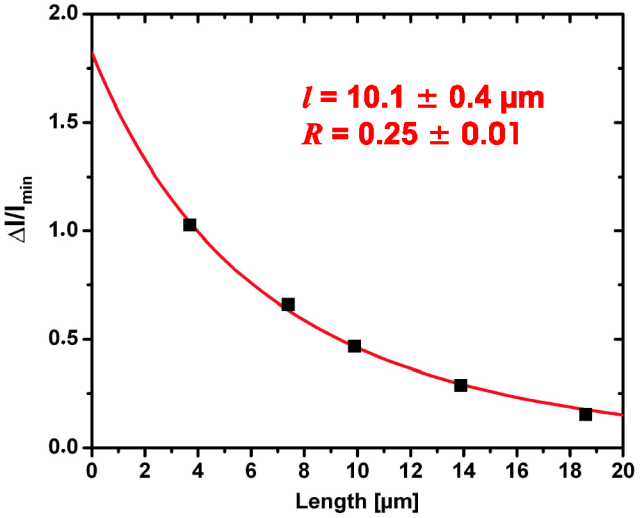

FIG. 5 (color online). Spectral modulation depth ($\Delta I/I_{\min}$) around a light wavelength of 785 nm versus nanowire length. The squares give the experimetal values for 5 nanowires with diameter 110 ± 15 nm. Line: Fit of the Fabry-Perot resonator model for determination of both the reflectivity of the wire end faces (R) and the propagation length of the plasmon mode (l).

damping, as illustrated by the nanowire plasmon dispersion relation in Fig. 6. This relation is deduced from the spectral data of the 18.6 μm long nanowire in Fig. 4(b) by assigning the plasmon mode numbers to the individual signal peaks, starting with the mode number 90 for the peak at a wavelength of 785 nm which was determined directly by SNOM [see Fig. 2(c)]. The dispersion relation is to the right of both light lines in air and in the glass substrate so that no direct coupling of plasmon and light can occur.

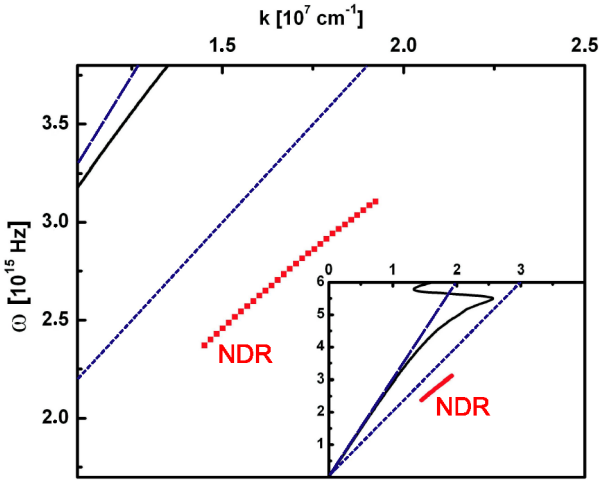

FIG. 6 (color online). Surface plasmon dispersion relation of a 120 nm diameter nanowire (NDR), as derived from the spectrum in Fig. 4(b). The solid black line is the surface plasmon dispersion relation at a flat silver/air interface. The long- and the short-dashed curves define the light lines in air and the glass substrate, respectively. Figure and inset show the same curves over different axes ranges.

In summary, we have shown that chemically prepared silver nanowires with a well developed crystal and surface structure sustain nonradiating surface plasmon modes with wavelengths shortened to about half the value of the exciting light. Accordingly, large propagation lengths of about 10 μm at a light wavelength of 785 nm and end face reflectivities of about 25% allow us to apply the nanowires as Fabry-Perot resonators. Such resonators could constitute a basic element for a variety of further nano-optical functionalities, as wavelength selectivity or applications in near-field optical lithography and microscopy.

Financial support is acknowledged from *Zukunftsfonds des Landes Steiermark* and the EU under Projects No. FP6 NMP4-CT-2003-505699 and No. FP6 2002-IST-1-507879.

[1] W. L. Barnes, A. Dereux, and T. W. Ebbesen, Nature (London) **424**, 824 (2003).
[2] P. Berini, Opt. Lett. **24**, 1011 (1999).
[3] B. Lamprecht, J. R. Krenn, G. Schider, H. Ditlbacher, M. Salerno, N. Felidj, A. Leitner, F. R. Aussenegg, and J. C. Weeber, Appl. Phys. Lett. **79**, 51 (2001).
[4] J.-C. Weeber, Y. Lacroute, and A. Dereux, Phys. Rev. B **68**, 115401 (2003).
[5] J. C. Ashley and L. C. Emerson, Surf. Sci. **41**, 615 (1974).
[6] J. Takahara, S. Yamagishi, H. Taki, A. Morimoto, and T. Kobayashi, Opt. Lett. **22**, 475 (1997).
[7] R. M. Dickson and L. A. Lyon, J. Phys. Chem. B **104**, 6095 (2000).
[8] J.-C. Weeber, A. Dereux, C. Girard, J. R. Krenn, and J. P. Goudonnet, Phys. Rev. B **60**, 9061 (1999).
[9] J. R. Krenn, B. Lamprecht, H. Ditlbacher, G. Schider, M. Salerno, A. Leitner, and F. R. Aussenegg, Europhys. Lett. **60**, 663 (2002).
[10] J.-C. Weeber, Y. Lacroute, A. Dereux, E. Devaux, T. Ebbesen, C. Girard, M. U. González, and A.-L. Baudrion, Phys. Rev. B **70**, 235406 (2004).
[11] T. Nikolajsen, K. Leosson, and S. I. Bozhevolnyi, Appl. Phys. Lett. **85**, 5833 (2004).
[12] H. Raether, *Surface Plasmons*, edited by G. Höhler, Springer Tracts Mod. Phys. Vol. 111 (Springer, Berlin, 1988).
[13] A. Graff, D. Wagner, H. Ditlbacher, and U. Kreibig, Eur. Phys. J. D **34**, 263 (2005).
[14] D. W. Pohl, W. Denk, and M. Lanz, Appl. Phys. Lett. **44**, 651 (1984).
[15] A. Lewis, M. Isaacson, A. Harootunian, and A. Murray, Ultramicroscopy **13**, 227 (1984).
[16] K. Karrai and R. D. Grober, Appl. Phys. Lett. **66**, 1842 (1995).
[17] L. Bergmann and C. Schaefer, *Optik* (Gruyter, Berlin, 1993), 9th ed.
[18] *Handbook of Microlithography, Micromachining and Microfabrication*, edited by M. A. McCord and M. J. Rooks (SPIE and The Institution of Electrical Engineers, Bellingham, WA, 1997), Vol. 1, pp. 139–249.